ADVANCES IN ATMOSPHERIC SCIENCES, VOL. 31, MARCH 2014, 457–467

An Analysis of Historical and Future Temperature Fluctuations over China Based on CMIP5 Simulations

LIU Yonghe[1], FENG Jinming*[2], and MA Zhuguo[2]

[1]*Institute of Resources and Environment, Henan Polytechnic University, Jiaozuo* 454000
[2]*Key laboratory of Regional Climate-Environment Research for Temperate East Asia, Institute of Atmospheric Physics, Chinese Academy of Sciences, Beijing* 100029

(Received 10 May 2013; revised 13 July 2013; accepted 17 July 2013)

ABSTRACT

The trends and fluctuations of observed and CMIP5-simulated yearly mean surface air temperature over China were analyzed. In general, the historical simulations replicate the observed increase of temperature, but the multi-model ensemble (MME) mean does not accurately reproduce the drastic interannual fluctuations. The correlation coefficient of the MME mean with the observations over all runs and all models was 0.77, which was larger than the largest value (0.65) from any single model ensemble. The results showed that winter temperatures are increasing at a higher rate than summer temperatures, and that winter temperatures exhibit stronger interannual variations. It was also found that the models underestimate the differences between winter and summer rates. The ensemble empirical mode decomposition technique was used to obtain six intrinsic mode functions (IMFs) for the modeled temperature and observations. The periods of the first two IMFs of the MME mean were 3.2 and 7.2, which represented the cycle of 2–7-yr oscillations. The periods of the third and fourth IMFs were 14.7 and 35.2, which reflected a multi-decadal oscillation of climate change. The corresponding periods of the first four IMFs were 2.69, 7.24, 16.15 and 52.5 in the observed data. The models overestimate the period of low frequency oscillation of temperature, but underestimate the period of high frequency variation. The warming rates from different representative concentration pathways (RCPs) were calculated, and the results showed that the temperature will increase by approximately 0.9°C, 2.4°C, 3.2°C and 6.1°C in the next century under the RCP2.6, RCP4.5, RCP6.0 and RCP8.5 scenarios, respectively.

Key words: CMIP5, surface air temperature, representative concentration pathways, warming rate, ensemble empirical mode decomposition

Citation: Liu, Y. H., J. M. Feng, and Z. G. Ma, 2014: An analysis of historical and future temperature fluctuations over China based on CMIP5 simulations. *Adv. Atmos. Sci.*, **31**(2), 457–467, doi: 10.1007/s00376-013-3093-0.

1. Introduction

Over the last century, the global mean surface air temperature (SAT) has increased by $0.74^{\circ}\mathrm{C} \pm 0.18^{\circ}\mathrm{C}$ (IPCC, 2007), and the mean increase in China has been 0.79°C, at a rate of 0.08°C (10 yr)$^{-1}$ (Tang and Ren, 2005; Li et al., 2010). In the latter half of the century (1951–2001), the mean rate of increase over China is estimated to have been 0.22°C (10 yr)$^{-1}$ (Ren et al., 2005).

It is important to understand how SAT will change over the next century so that informed decisions can be made relating to economic development and greenhouse gas emissions. Global climate models are the primary tool for estimating the impact of anthropogenic climate change. Zhou and Yu (2006) analyzed the comparative skills of 19 different coupled climate models by attempting to reproduce historical SAT over China in the 20th century. However, uncertainties in global models are a limiting factor in the estimation of air temperature, in particular on local scales. Nevertheless, a new generation of more complex models running future scenarios for the recently published Intergovernmental Panel on Climate Change Fifth Assessment Report (IPCC AR5) is widely expected to provide more certain projections. Furthermore, the fifth phase of the Coupled Model Intercomparison Project (CMIP5) provided a new set of coordinated climate model experiments (Taylor et al., 2012) in a multi-model context, enabling researchers to examine climatic predictability of air temperature changes for future scenarios based on similar forces. The coordinated experiments, in which many different climate models run a set of scenarios, are regarded as benchmarks for producing climate projections. CMIP5 uses historical runs (from the mid-1800s to 2005) to evaluate a model's performance against present climate and observed climate change, and uses four Representative Concentration Pathways (RCPs) for future climate scenarios. These RCPs begin in 2006 and continue to the end of the present century. The RCPs are labeled RCP2.6, RCP4.5, RCP6 and RCP8.5,

* Corresponding author: FENG Jinming
Email: fengjm@tea.ac.cn

according to the approximate target radiative forcing in the year 2100 (Meinshausen et al., 2011). For example, RCP4.5 identifies a concentration pathway that approximately results in a radiative forcing of 4.5 W m^{-2} in the year 2100, relative to pre-industrial conditions.

The temperature changes in multi-model CMIP5 simulations have been investigated in many studies, such as Diffenbaugh and Giorgi (2012), Jia and DelSole (2012), Sakaguchi et al. (2012); Xu and Xu (2012a, 2012b), and Yao et al. (2012). Similarly, there have been many investigations into forecasted temperature change over China based on CMIP3 datasets, for example by Xu et al. (2007), Xu et al. (2009a).

In the present paper, the estimated temperature changes from historical simulations and prediction simulations under different forcing pathways over China are analyzed, to investigate and compare model performance on different time scales. The study focuses mainly on the closeness of simulations to observations, annual or decadal fluctuations, warming rates, and seasonal characteristics.

2. Data and methods

2.1. *Data*

The monthly mean SAT (denoted by the variable "tas") data were obtained from the CMIP5 website. The data contain more than 50 model runs made by more than 20 models, and comprise historical simulations and forecasts using the scenarios of RCP2.6, RCP4.5, RCP6.0 and RCP8.5. The models are listed in Table 1. Among all the models, BNU-ESM, FGOALS2-s, BCC-CSM1.1 are developed by institutes in China. The models BNU-ESM, CanESM2, CESM, MIROC-ESM, NorESM-M, MPI-ESM-LR, and FIO-ESM are Earth system models, and the others are generally global climate models or coupled atmospheric and oceanic general circulation models (e.g., HADGEM2-AO). The resolutions of the data vary between $1.0° \times 1.0°$ and $3.0° \times 3.0°$ for different models.

Despite there being some inconsistencies between models (e.g., some of the required simulations are not available for all models and some models are run as an ensemble), we acquired as much data as possible for the present study. To compare with the SAT in CMIP5 simulations, the Climatic Research Unit (CRU) TS (time-series) 3.10 near-surface temperature data (Jones and Moberg, 2003; Simmons et al., 2004), produced by the British Atmospheric Data Center from 1900 to 2009, are used as a proxy for observed SAT. The resolution of the CRU data is $0.5° \times 0.5°$. Xu et al. (2009b) and Wu and Gao (2013) recently developed new temperature datasets over China, which are claimed to be of high quality. However, these new datasets cover a period from 1961 to 2009, which is not long enough for use in the present study.

Annual time series of mean SAT over the land region of China were calculated from the CMIP5 simulations and CRU data. The temperature value of each year is a weighted mean across all grid points in China, where the weight of each grid

Table 1. The models producing CMIP5 simulations

Model Name	Model Center	Resolution (lon×lat)
Australian Community Climate and Earth System Simulator 1.0 (ACCESS1.0)	The Centre for Australian Weather and Climate Research	192×145
Beijing Normal University –Earth System Model	College of Global Change and Earth System Science, Beijing Normal University	128×64
The Second Generation Canadian Earth System Model (CanESM2)	Canadian Centre for Climate Modelling and Analysis	128×64
Community Climate System Model version 4 (CCSM4)	National Center for Atmospheric Research	288×192
Flexible Globa1 Ocean-Atmosphere-Land System Model spectral version 2 (FGOALS–s2)	State Key Laboratory of Numerical Modeling for Atmospheric Sciences and Geophysical Fluid Dynamics, Institute of Atmospheric Physics，Chinese Academy of Sciences	128×108
Institute of Numerica1 Mathematics Climate Model version 4 (INMCM4)	Institute of Numerical Mathematics Russian Academy of Sciences	180×120
Model for Interdisciplinary Research on Climate version 5 (MIROC5)	Japan Agency for Marine-EaCh Science and Technology (JAMSTEC), Atmosphere and Ocean Research Institute，The University of Tokyo(AORI), and National Institute for Environmental Studies(NIES)	256×128
Mode1 for Interdisciplinary Research on Climate-Earth System (MIROC-ESM)	Japan Agency for Marine-EaCh Science and Technology (JAMSTEC), Atmosphere and Ocean Research Institute，The University of Tokyo(AORI), and National Institute for Environmental Studies(NIES)	128×64
Meteorological Research Institute Coupled General Circulation Model version 3 (MRI-CGCM3)	Meteorological Research Institute, Japan Meteorological Agency	320×160
The Norwegian Earth System Model with Intermediate Resolution(NorESM1-M)	Norwegian Climate Centre	144×96
The Beijing Climate Center Climate model version 1.1 (BCC-CSM 1.1)	The Beijing Climate Center	128×64
Hadley Centre Global Environmental Model version 2 -atmosphere –ocean (HADGEM2-AO)	Met Office Hardley Center	192×145

point is determined by its land area.

2.2. *Methods*

The special technique of ensemble empirical mode decomposition (EEMD) (Huang and Wu, 2008; Wu and Huang, 2009) was used for data analysis. EEMD is an improvement over the empirical mode decomposition (EMD) method (Huang et al., 1998). It is similar to the windowed Fourier transformation or wavelet transformation, but is more suitable for analyzing nonlinear and non-stationary time series. The EMD/EEMD method has been widely used in geophysical applications (Qian et al., 2011a, 2011b; Franzke, 2012; Li et al., 2012; Qin et al., 2012; Zhu et al., 2012). Unlike wavelet transformation, which obtains coefficients at all frequencies in a whole scale range (for continuous wavelet transformation) or at frequencies with equal intervals (for discrete wavelet transformation), EEMD decomposes the time series into a number of intrinsic mode functions (IMFs). The IMFs correspond to clearly separable and definable timescales that are empirically and adaptively decomposed according to the scale properties in the raw series. When processing a time series, the EEMD method produces several IMFs. Each IMF is a new series, which has the same length as the raw time series. The first IMF is the mode with the highest frequency and subsequent IMFs represent increasingly lower frequencies until the last IMF, which is the residual and demonstrates the main trend of the raw data.

In the present paper, each yearly mean SAT series over the whole China region was processed by EEMD, to allow us to investigate the differences between multiple CMIP5 simulations.

3. Results and discussion

3.1. *Direct comparison of the historical experiments*

3.1.1. *Trend of temperature change*

The ensemble mean SAT over all the simulations was calculated. From Fig. 1a, it is clear that the model-simulated temperature captures the main temperature fluctuations, but

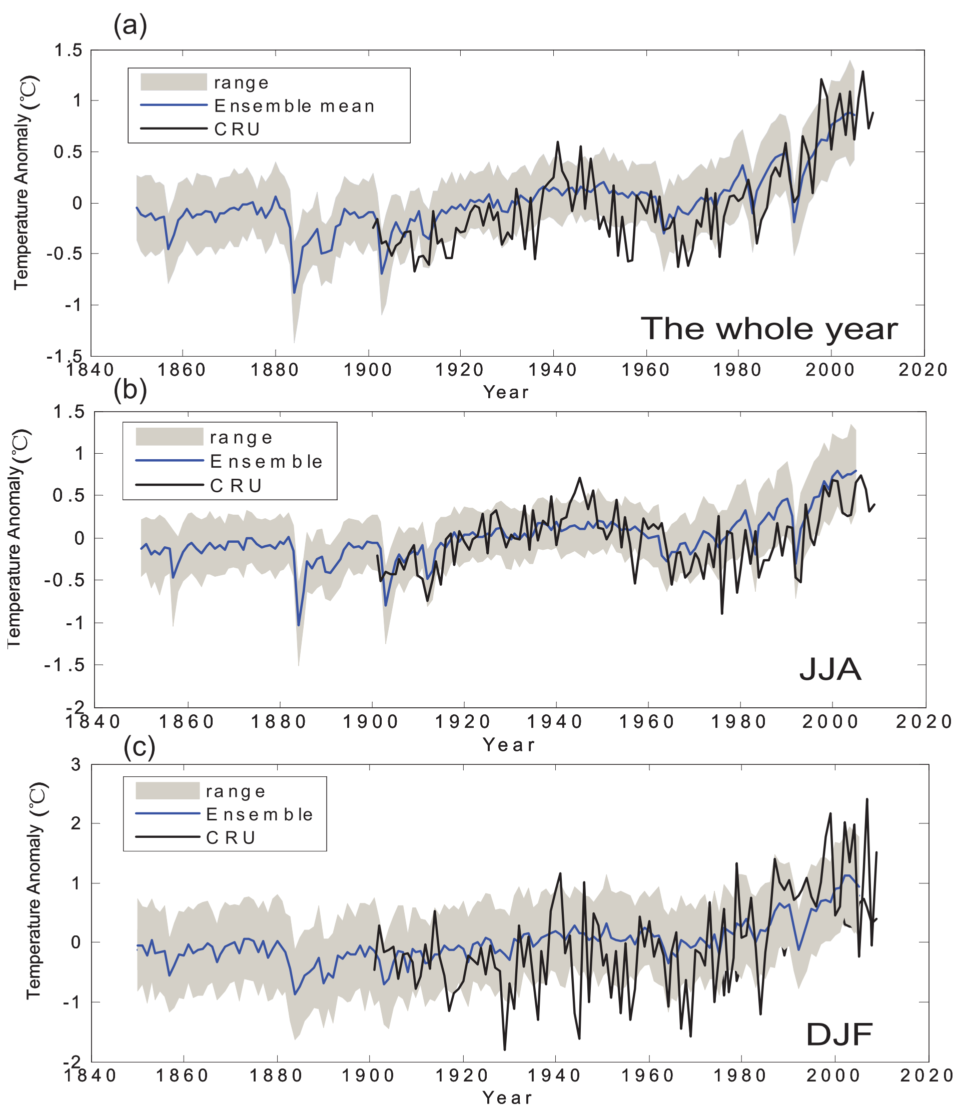

Fig. 1. Comparison of CMIP5-simulated temperature anomalies with those from CRU data.

the amplitudes are small when compared to observations. The CRU data show three distinct periods: 1900–50, 1950–70 and 1970 to present. The temperature increases in both the first period (1900–50) and the third period (1970 to present), but decreases in the second period (1950–70). Note that the third period spans more than 40 years, which is longer than the second period. Furthermore, in this last period, the temperature over China is extraordinarily higher than at any other time, particularly in recent years. The CMIP5 model simulations also exhibit this trend, but do not accurately predict the slope of the post-1970s increase. On a shorter time scale, the cold periods of 1900–20, 1950–60, 1967–70 and 1984 are very significant in the CRU data. While the simulated ensemble means have corresponding cold periods, the high peaks or deep troughs in observations are not well represented, and so the high frequency fluctuations are not well modeled. Some of the models do appear to be able to accurately forecast the extreme nature of some cold periods, but not the correct time.

According to the CRU temperature in Fig. 1b, the summer-high temperature peaks in the 20 years following 1990 appear somewhat comparable to the peaks in the 1940s. This suggests that the increase in summer temperatures is not as significant as annual temperatures. In the CMIP5 simulations, despite some deep drops over very short time periods, the increasing temperature trend is much stronger after 1990 than it is in the 1940s. This means that the comparatively weak warming increasing trend in June–July–August (JJA) is not well modeled.

For winter temperature, the CMIP5 simulations display similar trends as summer temperatures, except that the winter fluctuations seem larger than summer and annual fluctuations. The simulated fluctuations are not comparable to the very large fluctuations in the CRU data.

3.1.2. *Correlation coefficients of yearly series*

To quantify the performance of the simulations from different models, the correlation coefficients (R) of the yearly SAT series (1901–2005) of each model with the CRU temperature were calculated, with the results shown in Table 2. The R values of annual series range from 0.19 to 0.69 and have a mean value of 0.50. The HadGEM2-AO, INMCM4 and MIROC5 models yielded the smallest R values of approximately 0.4. The R values larger than 0.6 were produced by the single run of BNU-ESM (0.62), three runs of CCSM4 (0.63–0.65), one run of CSIRO-Mk (0.62), two runs of FGOALS (0.61, 0.68) and two runs of BCC-CSM1.1 (0.61, 0.64). It is worth noting that the runs of those models developed by institutes in China gave the comparatively larger R values.

When the ensemble mean of a single model was considered, the R values were larger than almost all of the single runs. The overall ensemble mean over all runs and all models obtained a correlation of 0.77, which was overwhelmingly larger than any value from single model ensembles.

The correlation coefficients for JJA and December–January–February (DJF) indicated that both their values were smaller than that calculated from the annual series. The R values for the ensemble from all runs and models were 0.57 and 0.46 for JJA and DJF, respectively.

3.1.3. *Seasonal characteristics*

According to some previous studies, the warming trend is more significant for winter temperatures than for summer temperatures. This phenomenon is also present in the CRU data (see Fig. 1). Comparing JJA, DJF and the whole year (Figs. 1a–c), the highest to lowest warming rates in CMIP5 model-simulated SAT are in DJF (winter), the whole year, and then JJA (summer). However, this difference in warming rates is not as obvious in the CMIP5 simulations. When comparing the amplitude of fluctuations of summer, winter and annual temperatures, it is clear that the interannual fluctuation of winter temperature is stronger than for summer or annual temperature. This is the case for both the CRU temperature (see Fig. 1) and the CMIP5 simulations.

3.1.4. *Historical warming rates*

The warming rates between 1956 and 2005 were estimated for each single run and for the ensemble mean. Ren et al. (2005) reported the mean temperature warming rate over China between 1951 and 2001 to be 0.22°C (10 yr)$^{-1}$, while Li et al. (2010) found a rate of 0.26°C (10 yr)$^{-1}\pm$ 0.032°C (10 yr)$^{-1}$ over the period 1954–2006. In a recent study by the present authors, records from more than 570

Table 2. Warming rates and correlation coefficients between model runs and CRU temperature series.

Model	Number of runs	50-yr trends [°C (10 yr)$^{-1}$]	100-yr trends [°C (10 yr)$^{-1}$]	R range from single runs	Mean R from multiple runs	R ensemble mean
MME	—	0.17	0.07	—	—	0.773
CCSM4	6	0.24	0.11	0.52–0.65	0.6	0.710
CSIRO Mk-3.6.0	10	0.14	0.03	0.38–0.62	0.485	0.682
MRI-CGCM3	5	0.10	0.07	0.38–0.44	0.40	0.533
BCC-CSM1.1	3	0.18	0.09	0.56–0.64	0.60	0.714
CESM1-CAM5	3	0.17	0.04	0.44–0.55	0.50	0.633
FGOALS	3	0.32	0.18	0.55–0.68	0.62	0.682
MIROC-ESM	3	0.13	0.05	0.42–0.56	0.47	0.656
MIROC5	4	0.08	0.01	0.19–0.40	0.29	0.415
NorESM	3	0.17	0.06	0.42–0.57	0.51	0.658
HadGEM2-AO	1	0.15	0.00	—	0.38	—
CanESM2	1	0.26	0.05	—	0.57	—
ACCESS1.0	1	0.22	0.02	—	0.52	—
BNU-ESM	1	0.31	0.13	—	0.62	—
CESM1-BGC	1	0.23	0.10	—	0.55	—
INMCM4	1	0.13	0.07	—	0.41	—

weather stations between 1962–2011 were used to obtain a rate of 0.284 ± 0.142°C (10 yr)$^{-1}$.

In the present study, we found an average warming rate of 0.173°C (10 yr)$^{-1} \pm 0.075$°C (10 yr)$^{-1}$ for all of the single runs of CMIP5 and a warming rate of 0.248°C (10 yr)$^{-1}$ from the CRU data. No model run resulted in a negative warming rate. For the overall ensemble mean of all runs and all models, the warming rate was estimated to be 0.173°C (10 yr)$^{-1}$, which was equal to the average of all the single runs. Considering individual models, the highest rates were obtained by FGOALS [0.32°C (10 yr)$^{-1}$] and CCSM4 [0.24°C (10 yr)$^{-1}$]. The next highest rates were obtained by CESM1-CAM5, bcc-csm and NorESM with values of approximately 0.17°C (10 yr)$^{-1}$, which was close to the value of the overall ensemble mean. The lowest warming rates were obtained by MIROC5, with a value of 0.08°C (10 yr)$^{-1}$. The warming rates obtained from CMIP5 simulations were small compared to those from the observations, and we believe that this is due to the underestimation of the amplitudes of fluctuations.

The warming rates obtained from the overall ensemble mean were 0.163°C (10 yr)$^{-1}$ and 0.204°C (10 yr)$^{-1}$ for JJA and DJF, respectively, which were both smaller than the values of 0.2°C (10 yr)$^{-1}$ and 0.39°C (10 yr)$^{-1}$ obtained in a recent study by the present authors. The ensemble means of the models CCSM4, BNU-ESM, FGOALS, CanESM2 and bcc-csm1 obtained larger warming rates than the observed 0.2°C (10 yr)$^{-1}$ in JJA. In DJF, only the runs by ACCESS1 and CanESM2 were able to obtain warming rates larger than the observed 0.39°C (10 yr)$^{-1}$. The FGOALS model obtained comparatively large warming rates in DJF, but only one of three runs attained the observed warming rate of 0.39°C (10 yr)$^{-1}$. In summary, the majority of models underestimate the observed warming rates of the past 50 years.

In the past 100 years (1906–2006), considering all seasons, the warming rates obtained by the overall ensemble mean temperature of the CMIP5 simulations was 0.64°C (100 yr)$^{-1}$. This was smaller than the global warming rate of 0.74°C (100 yr)$^{-1}$ estimated by the IPCC (2007). The warming rates in JJA and DJF were estimated as 0.55°C (100 yr)$^{-1}$ and 0.80°C (100 yr)$^{-1}$, respectively. Out of 50 individual model runs, 12 obtained 100-yr warming rates larger than 1.0°C (100 yr)$^{-1}$. Those runs were produced by FGOALS, BNU-ESM, CCSM4 and bcc-csm. Three runs gave negative warming rates, but the magnitudes were very close to zero.

3.2. *EEMD decompositions for historical experiments*

3.2.1. *Periods of different IMFs*

The EEMD method is able to decompose raw series into IMFs with different periods. The periods are empirically determined according to the properties in the raw data; therefore, each IMF may not correspond to a fixed cycle length. In this study, each single run and ensemble mean from each model were processed using the EEMD algorithm. The period between 1901 and 2005 was selected. Each set of CMIP5 simulation data produced six IMFs, where the sixth IMF was the main temperature trend. Table 3 shows the details of the IMFs obtained from the simulations of 15 CMIP5 models. The first to the fifth IMF correspond to approximate periods at 3.16, 7.17, 14.70, 35.25 and 79.30 years. The standard deviation of these periods are 0.19, 0.73, 1.95, 8.33 and 19.70 years, respectively. The periods of IMF1 for all models are in the range of 2.84–3.5 years, and those of IMF2 are 5.83–8.4 years. The corresponding periods of the CRU data are 2.69 and 7.24. The periods of the third and fourth IMFs of the models are in the range of 11.67–19.09 and 26.25–52.5 respectively, corresponding to periods of 16.15 and 52.5 from the CRU data. It is known that the periods of the IMFs decomposed by the EEMD algorithm are not completely sta-

Table 3. Mean cycles of the IMFs, standard deviations of the IMF series and the increase of temperature between 1901 and 2005. Note that the standard deviations are calculated for each IMF. The increasing temperature from 1901 to 2005 is calculated by subtracting the first value from the last value.

	Cycles of IMFs				Standard deviations of IMFs					Increasing temperature
	IMF1	IMF2	IMF3	IMF4	IMF1	IMF2	IMF3	IMF4	IMF5	(from IMF6)
CRU	2.69	7.24	16.15	52.50	0.16	0.09	0.08	0.10	0.12	0.97
ACCESS1.0	3.04	6.77	17.50	26.25	0.23	0.12	0.10	0.08	0.10	0.73
BNU-ESM	3.50	7.24	12.35	26.25	0.29	0.14	0.11	0.09	0.14	1.66
CCSM4	3.23	7.78	14.00	30.00	0.15	0.11	0.06	0.06	0.20	1.71
CESM1	2.84	8.40	16.15	30.00	0.22	0.16	0.10	0.08	0.09	1.38
CESM1-CAM5	2.96	7.78	13.13	35.00	0.13	0.10	0.08	0.05	0.16	0.76
CSIRO-Mk3.6.0	3.28	8.40	15.00	52.50	0.06	0.06	0.04	0.08	0.14	0.51
CanESM2	3.44	5.83	14.00	42.00	0.23	0.09	0.09	0.06	0.23	1.33
FGOALS2-s	3.23	6.18	16.15	30.00	0.19	0.10	0.08	0.07	0.14	2.26
HadGEM2-AO	2.92	7.00	13.13	42.00	0.24	0.15	0.10	0.16	0.33	0.55
MIROC-ESM	3.13	7.24	15.00	35.00	0.13	0.08	0.05	0.09	0.13	0.75
MIROC5	3.39	6.77	19.09	35.00	0.12	0.08	0.05	0.07	0.14	0.28
MRI-CGCM3	3.04	6.36	14.00	35.00	0.13	0.07	0.06	0.06	0.13	0.99
NorESM1-M	3.04	7.50	13.13	52.50	0.14	0.09	0.05	0.05	0.12	0.78
BCC-CSM1.1	3.33	6.77	11.67	30.00	0.14	0.10	0.07	0.04	0.16	1.52
INMCM4	3.04	7.50	16.15	26.25	0.26	0.15	0.13	0.06	0.06	1.00
Mean of models	3.16	7.17	14.70	35.25	0.18	0.11	0.08	0.07	0.15	1.08
Range of models	2.84–3.5	5.83–8.4	11.67–19.09	26.25–52.5	0.06–0.29	0.06–0.16	0.04–0.13	0.04–0.16	0.06–0.33	0.28–2.26
MME	2.96	7.50	19.09	42.00	0.07	0.06	0.04	0.05	0.16	1.08

tionary. In fact, they are only stationary within a narrow range. Only the average values for each IMF of each model are presented. The periods of the first and second IMFs represent temperature oscillations of 2–7 years, and the periods of the third and fourth IMFs represent a multi-decadal oscillation of climate change. Most models are able to catch these frequency characteristics to some extent, but the majorities underestimate high frequency oscillations and overestimate one of the low frequency oscillations. The periods of the fourth and fifth IMFs vary widely across the models, but they correspond to very low frequencies that are hard to determine with a limited amount of data.

The standard deviation of an IMF can indicate the intensity of its signal. In descending order of standard deviations, the IMFs of the CRU data are 1, 5, 4, 2, 3 (see Table 3). The IMFs exhibit differing relative intensities for different models, but the first and fifth IMFs generally have the strongest intensities, while the third and fourth are the weakest. In summary, the CRU data also exhibit stronger high frequency signals of 2–3 years and weaker multi-decadal signals.

3.2.2. *Trend from historical experiments*

Figures 2 and 3 display the second to fifth IMFs from different models. Clearly, the IMFs from the majority of the models are consistent with the IMFs of the CRU temperature.

The second order IMFs are better represented by the mod-

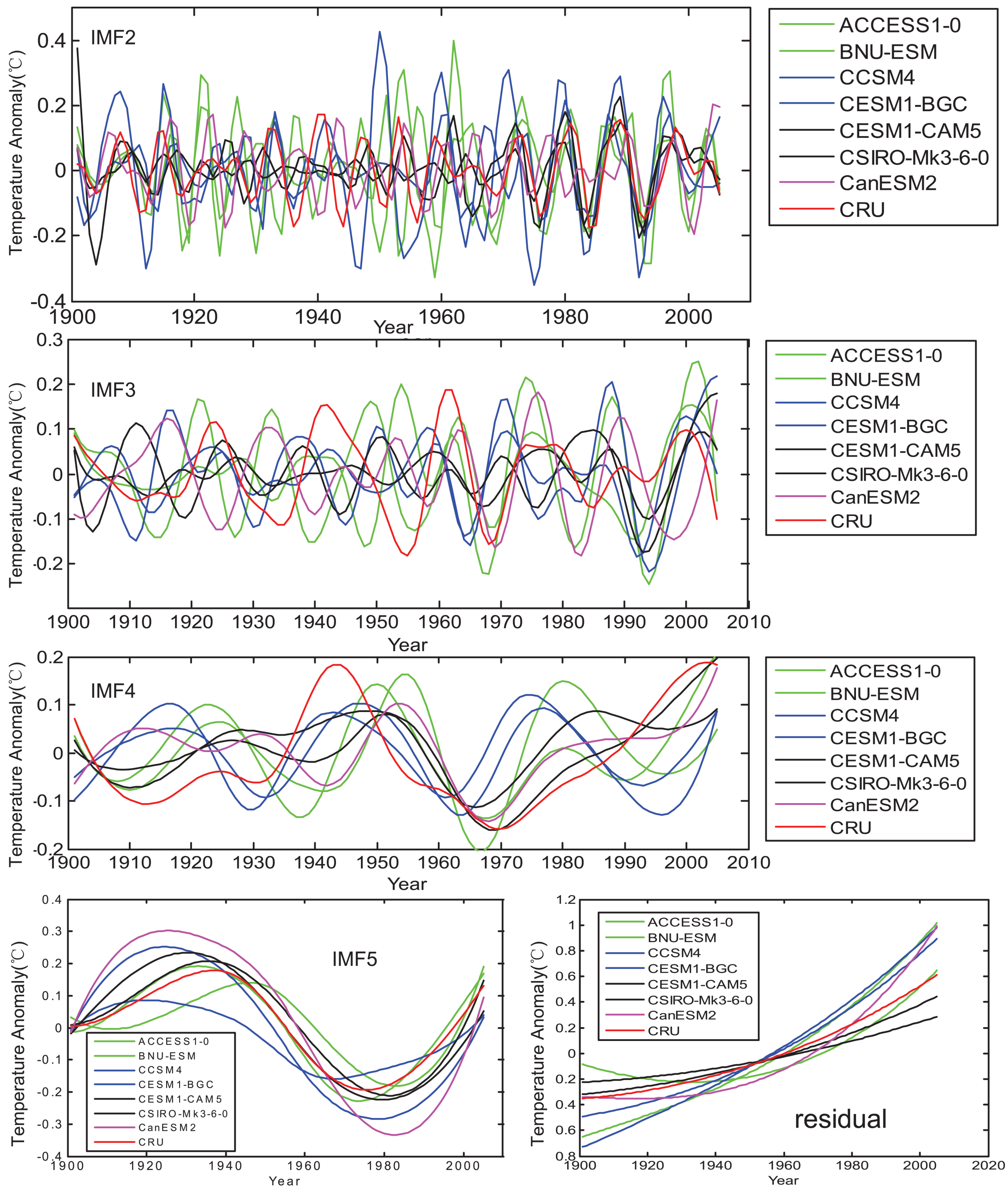

Fig. 2. The IMFs obtained from seven models of the CMIP5 simulations.

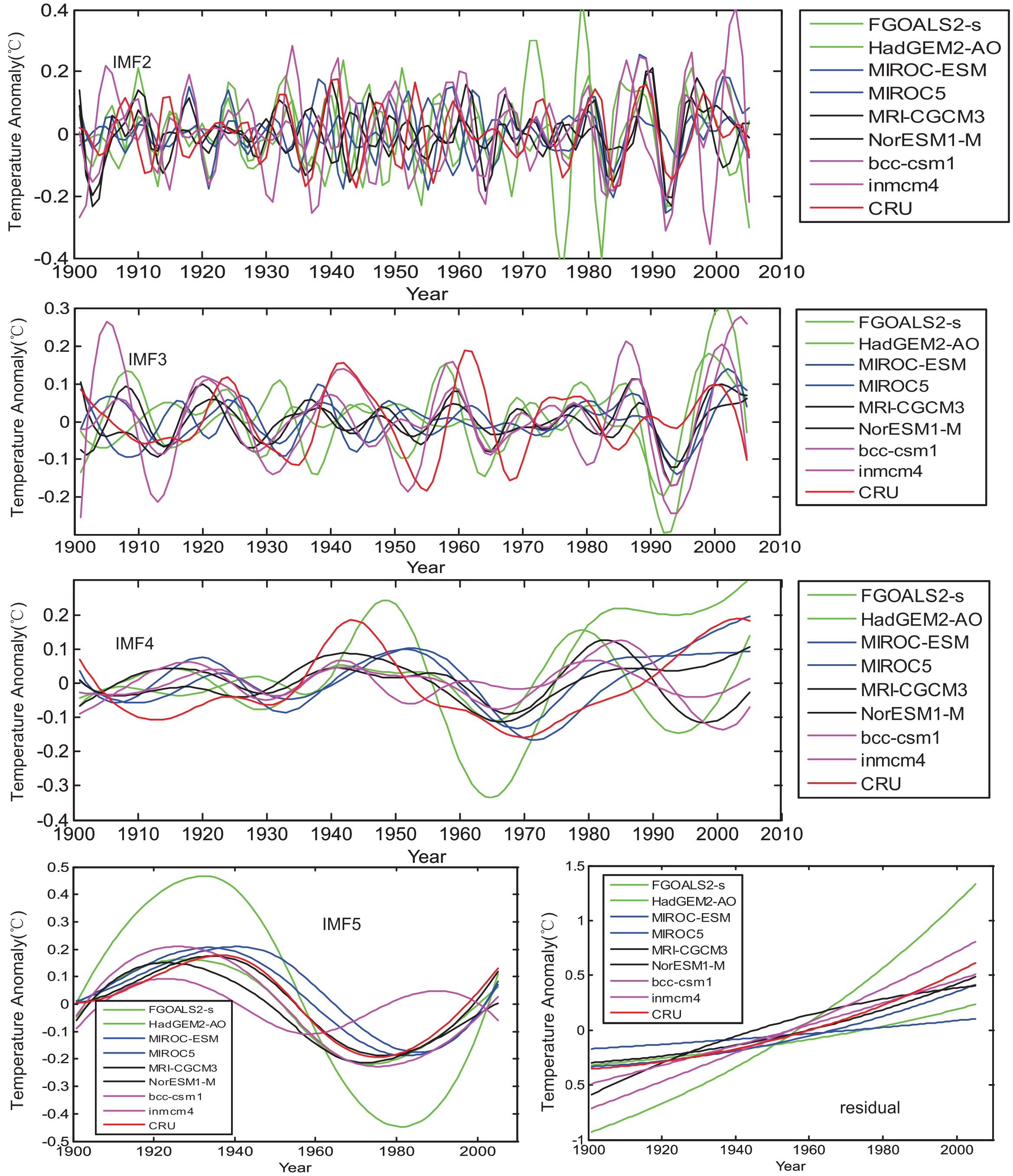

Fig. 3. The IMFs obtained from eight models of the CMIP5 simulations.

els than the third order IMFs. When only the second order IMFs are considered, the period from 1970 to 2005 is better represented than the period before 1970.

Comparing the fourth order IMFs over the last 30 years, the CRU series shows an increasing trend instead of the wave cycle that the majority of models suggest. Nevertheless, some models do simulate such a trend, such as CSIRO-MK, MIROC-ESM, and NorESM1-M. The CCSM4, CESM1-BGC, BNU-ESM, MRI-CGCM3, FGOALs and inmcm4 models show a strong wave cycle. However, other models exhibit weak cycles and a comparatively high temperature in the last 30 years, which corresponds somewhat to the increasing trend of the last three decades.

All of the models except for inmcm4 have a fifth order IMF that simulates a single wave cycle spanning the entire 105 years. The FGOALs model exhibits a single wave cycle, but with an amplitude far larger than that from other models and from the CRU temperature data. This exceptionally large amplitude does not occur in the other order IMFs of the same model.

The residuals of EEMD show an increasing trend for all models, but with different magnitudes. Among all the models, six have a rate larger than the CRU temperature. The historical warming suggested by the models between

1901 and 2005 was obtained directly from the sixth IMF (the residual) by subtracting the value at 1901 from the value at 2005 (see the last column in Table 3). The value obtained from the overall ensemble mean is close to the warming of 0.97°C calculated from the CRU temperature data. Ordering the models by temperature increase, from high to low, we get: FGOALS, CCSM4, BNU-ESM, BCC-CSM1.1, CESM1, CanESM2, INMCM4, MRI-CGCM3, NorESM1-M, CESM1-CAM5, MIROC-ESM, ACCESS1.0, HadGEM2-AO, CSIRO-Mk3.6.0 and MIROC5. The temperature increase calculated from the CRU data falls in the middle of these values. The increases calculated from MRI-CGCM3 and inmcm4 are closest to the value calculated from the CRU data. This result is not consistent with the directly estimated warming rates, which as previously discussed, underestimated the increase.

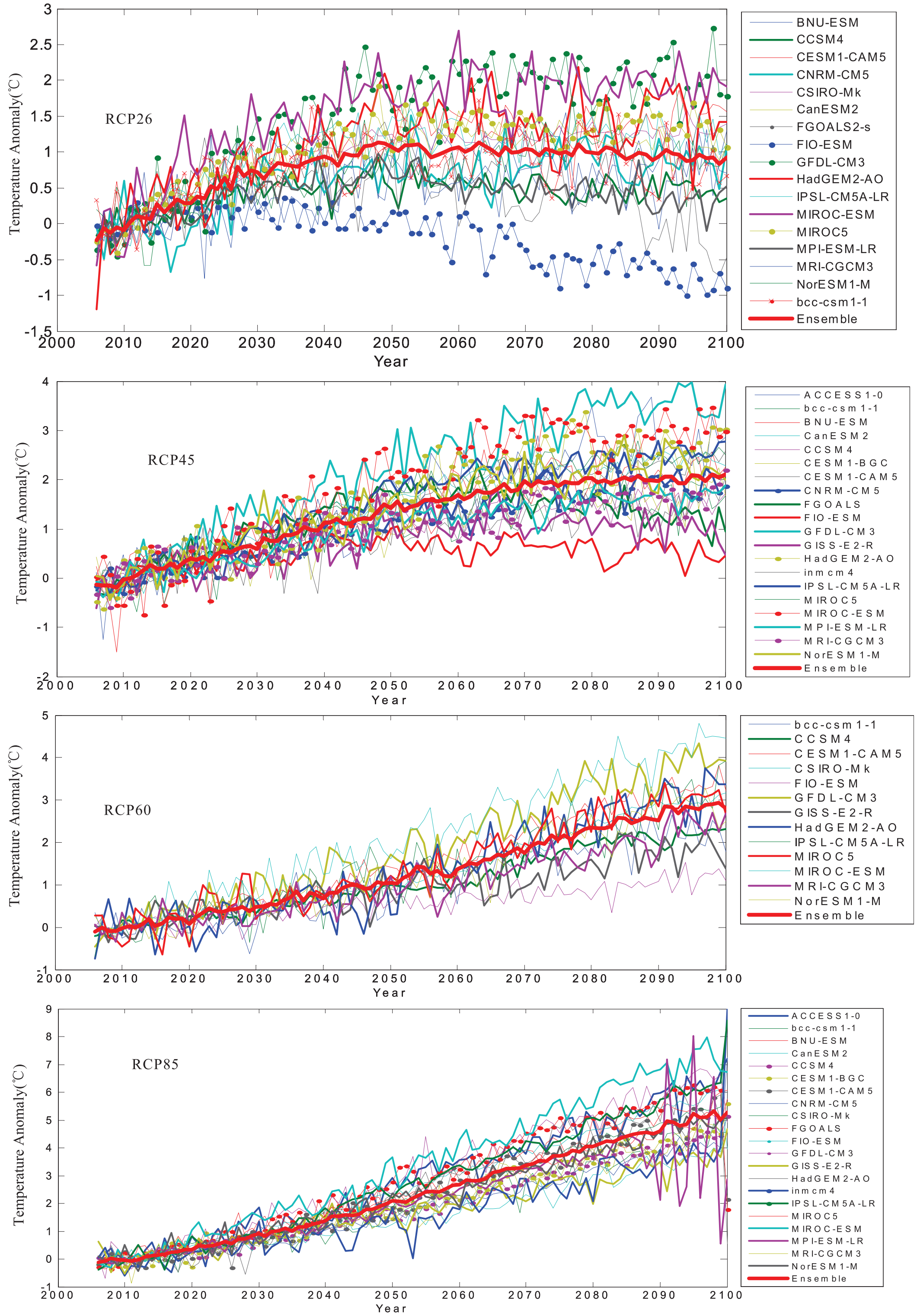

Fig. 4. SAT anomalies (relative to the mean of 2006–15) obtained from the model simulations under different RCPs.

3.3. *The warming rates for RCP experiments*

As shown in Fig. 4, the simulated SAT trends for each RCP have specific properties. For RCP2.6, the significant increase in temperature continues until 2030, where it peaks. After 2030, the temperature becomes stable and begins to slowly decrease or increase for different simulations. For RCP4.5, the significant temperature increase continues until approximately 2060, and is followed by a slower increase that continues until the end of the century. For RCP6.0, the increasing rate in the second half of the century is larger than that in the first half of the century. This high increasing rate decreases slightly near the end of the century. For RCP8.5, the warming rate remains high over the whole century.

Table 4 displays the ensemble mean warming rates of the four RCPs for the periods 2006–55, 2006–2100 and 2006–2300. They forecast that the temperature in this century could increase by approximately 0.9°C, 2.4°C, 3.2°C and 6.1°C for the RCP2.6, RCP4.5, RCP6.0, and RCP8.5 scenarios, respectively.

Under the scenario of RCP2.6, the largest warming rate of 0.26°C (10 yr)$^{-1}\pm$0.11°C (10 yr)$^{-1}$ was obtained for the period 2006–55. For the periods 2006–2100 and 2006–2300, the warming rates under RCP2.6 were close to 0.09°C (10 yr)$^{-1}$ and $-$0.01°C (10 yr)$^{-1}$. This means the scenario of RCP2.6 mostly influences the climate over the first half of the century. Similarly, the results for RCP4.5 forecast that there will be significant warming over the next 50 years, which will continue for 100 to 300 years, but with slowly decreasing warming rates.

However, the warming rates of RCP6.0 and RCP8.5 for 2006–55 are smaller than the period from 2006 until the end of this century. This indicates that the highest peak of warming rate will occur in the second half of the century. It is also clear that the warming rates in summer are slightly lower than in winter.

Table 5 displays the different warming rates for each model. The largest increasing rates were obtained by MIROC5, FGOALS, and HadGEM2-AO, and were near or larger than 0.8°C (10 yr)$^{-1}$ in the long-term period to 2100. The Earth system models (BNU-ESM, CanESM2, MIROC-ESM, NorESM1-M) obtained medium warming rates in the range of 0.5°C (10 yr)$^{-1}$–0.7°C (10 yr)$^{-1}$ (to 2100), but it is not clear whether these complex Earth system models produce more accurate predictions. Note that FIO-ESM obtained a low warming rate of 0.44°C (10 yr)$^{-1}$ (to 2100).

As discussed in previous sections, the majority of models underestimate the historical warming rate. If this is an indication of the accuracy of the different models, then the warming rates should be close to the results of models such as FGOALS. This suggests that the best forecast of the temperature increase over this century, for the four RCPs, should be larger than 3°C, 4°C, 5°C and 7°C. However, the models contain many uncertainties. The models CCSM4 and BNU-ESM exhibit larger warming rates in the last 50 years than other models, but they forecast a comparatively small increase for future scenarios. The model MIROC5 simulates very low historical warming rates, but gives very large increases under RCP8.5. Nevertheless, models such as FGOALS and BNU-ESM appear to give consistent results.

4. Conclusion

The performances of a number of different CMIP5 models in terms of their simulations of SAT over China were analyzed by examining their closeness to observed historical values. The study focused on the trend of fluctuations, seasonal characteristics and warming rates.

In general, the CMIP5 historical simulations captured the increase in temperature, particularly in the last 30 years, but the interannual fluctuations in the simulated grand ensemble mean were not as drastic as observed in the CRU data. The correlation coefficients between simulations and observations (CRU data) ranged from 0.194 to 0.688 with a mean of 0.5. The models HadGEM2-AO, inmcm4, and MIROC5 produced the smallest correlations (approximately 0.4). The models BNU-ESM, CCSM4, CSIRO-Mk, FGOALS and BCC-CSM1-1 exhibited the largest correlations with observations, with some runs resulting in correlation coefficients larger than 0.6. The simulations made by those models de-

Table 4. The mean and standard deviation of warming rates [units: °C (10 yr)$^{-1}$] over all runs and all models for different time periods.

Period		Whole year	JJA	DJF
2006–55	RCP26	0.26 ± 0.11	0.24 ± 0.11	0.26 ± 0.14
	RCP45	0.36 ± 0.10	0.36 ± 0.11	0.38 ± 0.12
	RCP60	0.26 ± 0.08	0.27 ± 0.10	0.28 ± 0.09
	RCP85	0.51 ± 0.11	0.53 ± 0.13	0.54 ± 0.13
2006–2100	RCP26	0.09 ± 0.08	0.08 ± 0.08	0.09 ± 0.09
	RCP45	0.24 ± 0.09	0.24 ± 0.09	0.25 ± 0.10
	RCP60	0.32 ± 0.10	0.32 ± 0.10	0.34 ± 0.10
	RCP85	0.61 ± 0.11	0.59 ± 0.21	0.67 ± 0.16
2006–2300	RCP26*	−0.014	−0.02	−0.014
	RCP45	0.07 ± 0.02	0.065 ± 0.015	0.07 ± 0.03
	RCP60	0.14	0.13	0.14
	RCP85	0.48 ± 0.16	0.41 ± 0.13	0.51 ± 0.17

*The runs were too few to calculate the standard deviations.

Table 5. The warming rates [units: °C (10 yr)$^{-1}$] from a single run or the ensemble mean of each model for 2006–55.

Model	2006–55				2006–2100			
	RCP26	RCP45	RCP6	RCP85	RCP26	RCP45	RCP6	RCP85
ACCESS1-0		0.39		0.64		0.35		0.75
bcc-csm1-1	0.22	0.31	0.27	0.41	0.59	0.29	0.30	0.52
BNU-ESM	0.23	0.29		0.54	0.80	0.25		0.66
CCSM4	0.15	0.26	0.23	0.41	0.35	0.19	0.28	0.52
CESM1-BGC		0.26		0.45		0.21		0.55
CESM1-CAM5	0.3	0.37	0.32	0.49	0.15	0.29	0.40	0.62
CNRM-CM5	0.25	0.31		0.38	0.17	0.25		0.51
CSIRO-Mk	0.31		0.25	0.51	0.14		0.36	0.66
CanESM2	0.31	0.4		0.59	0.11	0.29		0.68
FGOALS2	0.18	0.44		0.68	−0.39	0.14		0.80
FIO-ESM		0.19	0.15	0.33	−0.18	0.48	0.14	0.44
GFDL-CM3	0.51	0.58	0.41	0.7	0.23	0.43	0.46	0.76
GISS-E2-R			0.22	0.42		0.12	0.27	0.43
HadGEM2-AO	0.39	0.4	0.23	0.58	0.16	0.35	0.42	0.77
Inmcm4		0.21		0.28		0.19		0.49
IPSL-CM5A-LR	0.35	0.46	0.33	0.65	0.12	0.32	0.38	0.76
MIROC-ESM	0.43	0.56	0.48	0.55	0.19	0.39	0.53	0.59
MIROC5	0.34	0.45	0.28	0.75	0.14	0.38	0.37	0.85
MPI-ESM-LR	0.19	0.3		0.48	0.27	0.21		0.51
MRI-CGCM3	0.17	0.3	0.24	0.39	0.16	0.20	0.28	0.54
NorESM1-M	0.23	0.37	0.27	0.53	0.11	0.27	0.34	0.58

veloped at institutes in China produced comparatively larger correlation values. The comparison also highlighted that the correlation coefficient of the ensemble mean of each model is usually larger than that from a single run. Furthermore, the overall ensemble mean over all runs from all models obtained a correlation value of 0.77, which was overwhelming larger than any value from a single model. This characteristic indicates that no model is consistently more accurate than any other single model.

The CMIP5 simulations also reflected the characteristic of a larger increasing rate of winter temperature than that of summer temperature, but the contrast between summer and winter was not as significant as seen in the historical observations. The simulations also reflected the stronger interannual fluctuations of winter temperature than that of summer temperature.

The values of the CMIP5-modeled warming rates over the past 50 and 100 years highlighted a tendency to underestimate, although almost no negative trends appeared. Only a small number of models, such as ACCESS1, CanESM2 and FGOALS, obtained warming rates similar to the observed rate of 0.39°C (10 yr)$^{-1}$, as estimated in other previous studies by the present authors.

The technique of EEMD was used for processing the modeled and observed temperature series into six IMFs (the sixth order IMF being the residual) that corresponded to different periods. In general, the same order IMFs from different simulations displayed similar characteristics for similar time scales. The correlation coefficients between the same ordered IMFs of simulations and observations were also compared. The residuals from all the models accurately reflected the increasing trend and the sinusoidal IMF5 cycles. It is clear that the main temperature fluctuations of the last century comprised of two fluctuations of IMF5 and the residual.

The multi-model ensemble mean temperature series obtained a correlation coefficient larger than that from single models, but its IMFs did not produce better correlations than the single models. No model was able to accurately simulate all the IMFs of the observed temperature series.

The increase of SAT in the last 50 years from the sixth order IMF (the residual) was estimated by subtracting the first value from the last value. However, these values indicated the observed increase lies in the middle of the values predicted by the models, which is contrary to the results obtained by regression. The result from direct regression appears more consistent than the result from IMF residuals. However, it is not clear which one is more representative of reality because both techniques contain uncertainties.

The warming rates of simulations under different RCPs were calculated. For the RCP2.6 and RCP4.5 scenarios, the significant increase of temperature continues to 2030 and 2060, and is then followed by a lower rate of increase. For RCP6.0, the increasing rate in the second half of the century is larger than that in the first half, and decreases slightly near the end of the century. For RCP8.5, the increasing rate remains high throughout the century. The future warming rates estimated from these RCPs in summer are slightly smaller than in winter, and are consistent with the increase of annual temperature.

Acknowledgements. This study was jointly supported by the General Project of the National Natural Sciences Foundation of China (Grant Nos. 41105074 and 41275108), the Innovation Key Program of the Chinese Academy of Sciences (Grant No.

KZCX2-EW-202), the National Basic Research Program of China (2012CB956201), the Open Research Fund of the Key Laboratory of Digital Earth Science, Center for Earth Observation and Digital Earth, Chinese Academy of Sciences (Grant No. 2011LDE010), and the Scientific Research Fund of Henan Polytechnic University (Grant No. B2011-038).

REFERENCES

Diffenbaugh, N. S., and F. Giorgi, 2012: Climate change hotspots in the CMIP5 global climate model ensemble. *Climatic Change*, **114**(3–4), 813–822.

Franzke, C., 2012: Nonlinear trends, long-range dependence, and climate noise properties of surface temperature. *J. Climate*, **25**(12), 4172–4183.

Huang, N. E., and Z. H. Wu, 2008: A review on Hilbert-Huang transform: Method and its applications to geophysical studies. *Rev. Geophys.*, **46**(2), doi: 10.1029/2007RG000228.

Huang, N. E., and Coauthors, 1998: The empirical mode decomposition and the Hilbert spectrum for nonlinear and nonstationary time series analysis. *Proceedings of the Royal Society A*: *Mathematical, Physical and Engineering Sciences*, **454**(1971), 903–995.

IPCC, 2007: Climate change 2007: Synthesis report. *Contribution of Working Groups I, II and III to the Fourth Assessment Report.* Cambridge University Press, 104 pp.

Jia, L. W., and T. DelSole, 2012: Multi-year predictability of temperature and precipitation in multiple climate models. *Geophys. Res. Lett.*, **39**, doi: 10.1029/2012GL052778.

Jones, P. D., and A. Moberg, 2003: Hemispheric and large-scale surface air temperature variations: An extensive revision and an update to 2001. *J. Climate*, **16**, 206–223.

Li, F. L., Y. H. Jo, W. T. Liu, and X. H. Yan, 2012: A dipole pattern of the sea surface height anomaly in the North Atlantic: 1990s–2000s. *Geophys. Res. Lett.*, **39**, L15604, doi: 10.1029/2012GL052556.

Li, Q. X., and Coauthors, 2010: Assessment of the uncertainties in temperature change in China during the last century. *Chin. Sci. Bull.*, **55**, 1974–1982.

Meinshausen, M., and Coauthors, 2011: The RCP greenhouse gas concentrations and their extensions from 1765 to 2300. *Climatic Change*, **109**(1–2), 213–241.

Qian, C., C. B, Fu, and Z. H., Wu, 2011a: Changes in the amplitude of the temperature annual cycle in China and their implication for climate change research. *J. Climate*, **24**(20), 5292–5302.

Qian, C., Z. H., Wu, C. B. Fu, and D. X., Wang, 2011b: On changing El Nino: A view from time-varying annual cycle, interannual variability, and mean state. *J. Climate*, **24**(24), 6486–6500.

Qin, Z., X. Zou, and F., Weng, 2012: Comparison between linear and nonlinear trends in NOAA-15 AMSU-A brightness temperatures during 1998–2010. *Climate Dyn.*, **39**(7–8), 1763–1779.

Ren, G. Y., and Coauthors, 2005: Recent progresses in studies of regional temperature changes in China. *Climatic and Environmental Research*, **10**(4), 701–716. (in Chinese)

Sakaguchi, K., X. B. Zeng, and M. A. Brunke, 2012: The hindcast skill of the CMIP ensembles for the surface air temperature trend. *J. Geophys. Res.*, **117**, doi: 10.1029/2012JD017765.

Simmons, A. J., and Coauthors, 2004: Comparison of trends and low-frequency variability in CRU, ERA-40, and NCEP/NCAR analyses of surface air temperature. *J. Geophys. Res.*, **109**(D24), D24115, doi: 10.1029/2004JD005306.

Tang, G. L., and G. Y. Ren, 2005: Reanalysis of surface air temperature change of the last 100 years over China. *Journal of Arid Land Resources and Environment*, **10**(4), 791–798. (in Chinese)

Taylor, K. E., R. J., Stouffer, and G. A., Meehl, 2012: An overview of CMIP5 and the experiment design. *Bull. Amer. Meteor. Soc.*, **93**, 485–498.

Wu, J., and X. J. Gao, 2013: A gridded daily observation dataset over China region and comparison with the other datasets. *Chinese Journal Geophysics*, **56**(4), 1102–1111. (in Chinese)

Wu, Z. H., and N. E. Huang, 2009: Ensemble empirical mode decomposition: a noise-assisted data analysis method. *Adv. Adapt. Data Anal.*, **1**(1), 1–41.

Xu, C. H., and Y. Xu, 2012a: The projection of temperature and precipitation over China under RCP scenarios using a CMIP5 multi-model ensemble. *Atmos. Oceanic Sci. Lett.*, **5**, 527–533.

Xu, C. H., Y. X. Shen and Y., Xu, 2007: An analysis of climate change in East Asia by using the IPCC AR4 simulations. *Adv. Climate Change Res.*, **3**(5), 287–292.

Xu, Y., and C. H. Xu, 2012b: Preliminary assessment of simulations of climate changes over China by CMIP5 multi-models. *Atmos. Oceanic Sci. Lett.*, **5**, 489–494.

Xu, Y., X. J. Gao, and F. Giorgi, 2009a: Regional variability of climate change hot-spot in East Asia. *Adv. Atmos. Sci.*, **26**(4), 783–792, doi: 10.1007/s00376-009-9034-2.

Xu, Y., X. J. Gao, Y. Shen, C. H. Xu, Y. Shi, and F. Giorgi, 2009b: A daily temperature dataset over China and its application in validating a RCM simulation. *Adv. Atmos. Sci.*, **26**(4), 763–772, doi: 10.1007/s00376-009-9029-z.

Yao, Y., Y. Luo, and J. B. Huang, 2012: Evaluation and projection of temperature extremes over China based on 8 modeling data from CMIP5. *Progressus Inquisitiones De Mutatione Climatis*, **8**(4), 250–256.

Zhou, T. J., and R. C. Yu, 2006: Twentieth-century surface air temperature over China and the globe simulated by coupled climate models. *J. Climate*, **19**(22), 5843–5858.

Zhu, J. S., B. H. Huang, and Z. H. Wu, 2012: The role of ocean dynamics in the interaction between the Atlantic meridional and equatorial modes. *J. Climate*, **25**(10), 3583–3598.